



Phospholipase D1-generated phosphatidic acid modulates secretory granule trafficking from biogenesis to compensatory endocytosis in neuroendocrine cells

Emeline Tanguy, Alexander Wolf, Qili Wang, Sylvette Chasserot-Golaz, Stéphane Ory, Stéphane Gasman, Nicolas Vitale^{*}

Centre National de la Recherche Scientifique, Université de Strasbourg, Institut des Neurosciences Cellulaires et Intégratives, F-67000, Strasbourg, France

ARTICLE INFO

Keywords:

Exocytosis
Endocytosis
Fatty acid
Phosphatidic acid
Phospholipase D
Neuroendocrine secretion

ABSTRACT

Calcium-regulated exocytosis is a multi-step process that allows specialized secretory cells to release informative molecules such as neurotransmitters, neuropeptides, and hormones for intercellular communication. The biogenesis of secretory vesicles from the Golgi cisternae is followed by their transport towards the cell periphery and their docking and fusion to the exocytic sites of the plasma membrane allowing release of vesicular content. Subsequent compensatory endocytosis of the protein and lipidic constituents of the vesicles maintains cell homeostasis. Despite the fact that lipids represent the majority of membrane constituents, little is known about their contribution to these processes. Using a combination of electrochemical measurement of single chromaffin cell catecholamine secretion and electron microscopy of roof-top membrane sheets associated with genetic, silencing and pharmacological approaches, we recently reported that diverse phosphatidic acid (PA) species regulates catecholamine release efficiency by controlling granule docking and fusion kinetics. The enzyme phospholipase D1 (PLD1), producing PA from phosphatidylcholine, seems to be the major responsible of these effects in this model. Here, we extended this work using spinning disk confocal microscopy showing that inhibition of PLD activity also reduced the velocity of granules undergoing a directed motion. Furthermore, a dopamine β -hydroxylase (D β H) internalization assay revealed that PA produced by PLD is required for an optimal recovery of vesicular membrane content by compensatory endocytosis. Thus, among numerous roles that have been attributed to PA our work gives core to the key regulatory role in secretion that has been proposed in different cell models. Few leads to explain these multiple functions of PA along the secretory pathway are discussed.

1. Introduction

The secretory pathway is an essential cellular function requiring synthesis, modification, sorting and release of secretory proteins/molecules outside of cells, as well as transport of their surface components. This secretory pathway is either constitutive, for molecules involved in maintaining cellular homeostasis, or regulated to allow cells to release informative molecules to neighboring cells or in the

^{*} Corresponding author.

E-mail address: vitalen@unistra.fr (N. Vitale).

blood circulation in a highly controlled manner. The regulated pathway is a trademark of specialized secretory cells such as neurons, endocrine and exocrine cells, and requires accumulation of secretory material into dedicated organelles: secretory vesicles (Vázquez-Martínez et al., 2012). Those vesicles are subsequently transported through the cytoplasm towards the cell periphery, where their journey climax after docking and fusion with the plasma membrane to release their content after cell stimulation (Burgess and Kelly, 1987). Finally the constituents of vesicular membrane inserted in the plasma membrane are recycled by compensatory endocytosis (Gasman and Vitale, 2017).

Over the last decades, discovery of the minimal fusion machinery and identification of numerous regulators has given us a relatively good understanding of the key protein players involved in those processes (Rizo and Xu, 2015). This appears important as it is now appreciated that alterations of some of these actors directly lead to numerous human pathologies (Verhage and Sørensen, 2020). However, in addition to the function of important protein players in the journey of secretory vesicles, lipids also contribute to key steps. Cell membranes are indeed composed of a broad spectrum of those aliphatic molecules whose specific properties can directly influence membrane topology, dynamics, and tasks. In addition, the lipid composition and the transbilayer arrangement of specific organelles can vary greatly and there is compelling evidence that the collective properties of bulk lipids profoundly define their identity and function (Holthuis and Menon, 2014). Of particular interest are changes in the physical properties of membranes that are directly under the control of lipids, and mark the transition from early to late organelles in the secretory pathway. These include bilayer thickness, lipid packing density and surface charge (Bigay and Antonny, 2012).

Regarding the role of lipids in regulated exocytosis, the two best-studied are without a doubt cholesterol and phosphoinositids (PI) (Tanguy et al., 2016). For instance, tempering with cholesterol and PI(4,5)P₂ levels considerably affected exocytosis in many secretory cell models (Ammar et al., 2013b; Gasman and Vitale, 2017; Katan and Cockcroft, 2020). More recently, membrane-permeant photoactivatable PI(4,5)P₂ combined with electrophysiological measurements in mouse adrenal chromaffin cells, identified the Ca²⁺ sensor for exocytosis synaptotagmin-1 and the vesicle priming protein Munc13-2 as relevant effector proteins (Walter et al., 2017). Furthermore, *in vitro* lipid nanodiscs experiments indicated that cholesterol dramatically stabilizes fusion pores in the open state by increasing membrane bending rigidity, without affecting its size (Wu et al., 2021). Intriguingly, manipulation of phospholipids to increase membrane stiffness mirrored the effects of cholesterol, suggesting that cholesterol is altering the elastic properties of lipid bilayers. Among phospholipids, PA is an important intermediate metabolite in the synthesis of all membrane glycerophospholipids, hence playing an important structural role in living cells by contributing to membrane biogenesis. However, more recently, important signaling functions have been attributed to this lipid and PA has thus also attracted some attention (Jenkins and Frohman, 2005; Tanguy et al., 2018). PA consists of a glycerol backbone to which are attached, through esterification, two fatty acyl chains and a phosphate at positions *sn*-1, *sn*-2, and *sn*-3, respectively. A specific feature of PA compared to other phospholipids is its small anionic phosphate headgroup. Therefore, this phospholipid has been predicted by X-ray diffraction studies to adopt a cone-shaped structure in membranes (Kooijman et al., 2005). This confirmed the ability of PA to modify membrane topology by creating a negative curvature. Accordingly this property is often linked to its contribution in diverse membrane trafficking events (Ammar et al., 2013b; Tanguy et al., 2016). Moreover, PA serves also as an essential signaling molecule in diverse cellular processes, through the recruitment of a broad range of cytosolic proteins to appropriate membrane locations (Kim and Wang, 2020).

The requirement of PA in calcium-regulated exocytosis in neuroendocrine and endocrine cells is one of the best documented role for this phospholipid in membrane trafficking (Bader and Vitale, 2009; Bowling et al., 2021). The inhibitory action of butanol on PA synthesis by phospholipase D (PLD) and on exocytosis from chromaffin cells was the first argument in favor for a contribution of PLD in neuroendocrine secretion (Caumont et al., 1998; Galas et al., 1997). These observations have since been validated in various cell models (Bullen et al., 2019; Choi et al., 2002; Holden et al., 2011; Hughes et al., 2004; Marchini-Alves et al., 2015; O'Lunaigh et al., 2002). PLD's overexpression or silencing experiments further supported the notion that the isoform PLD1 is the major source for PA synthesis during exocytosis in chromaffin cells (Zeniou-Meyer et al., 2007). Additional studies highlighted a tight regulation of PLD1 activity by several upstream signaling pathways involving small GTPases and the kinase RSK2 (Bader and Vitale, 2009; Zeniou-Meyer et al., 2008). Furthermore, PA was shown to be critical for SNARE complex assembly and to play a peculiar function for fusion in an *in vitro* setup (Mima and Wickner, 2009). More recently, a combination of genetic and pharmacological approaches associated with carbon fiber amperometry and electron microscopy imaging on roof-top membrane sheet preparations revealed that PA generated by PLD1 is actively involved in secretory granule docking and fusion steps (Tanguy et al., 2021). Among the six members of the PLD family, PLD1 and PLD2 are the best characterized (Frohman, 2015). Here we investigated the potential contribution of PLD1 enzymatic activity along additional steps of the secretory pathway.

2. Material and methods

Animals. *Pld1* knockout mice were described previously and the efficiency of knockout established (Ammar et al., 2013a, 2015). They were housed and raised at Chronobiotron UMS 3415. All experiments were carried out in accordance with the European Communities Council Directive of November 24, 1986 (86/609/EEC) and resulting French regulations. Accordingly, the CREMEAS local ethical committee approved all experimental protocols. Every effort was made to minimize the number of animals used and their suffering.

Transmission electron microscopy of chromaffin cells. Wild-type, *Pld1*^{-/-} and *Pld2*^{-/-} mice were anesthetized with a mixture of ketamine (100 mg/kg) and xylazine (5 mg/kg) and transcardially perfused with 0.1 M phosphate buffer, pH 7.3, containing 2% paraformaldehyde and 2.5% glutaraldehyde. 2-mm-thick slices were cut from the adrenal glands and postfixed in 1% glutaraldehyde in phosphate buffer overnight at 4 °C. The slices were then immersed for 1h in phosphate buffer containing OsO₄ 0.5%. 1-mm³ blocks were cut in the adrenal medulla, dehydrated, and processed classically for embedding in Araldite and ultramicrotomy. Ultrathin

sections were counterstained with uranyl acetate and examined with a Hitachi 7500 transmission electron microscope. Secretory granules were counted in 50 chromaffin cells from WT and *Pld1*^{-/-} mice each with a visible nucleus randomly selected in ultrathin sections from several blocks (1 section/block) from each mouse. Secretory granule diameters were measured from WT and KO cells using the line segment tool in ImageJ. Samples were blinded to minimize bias measurements.

Primary culture of chromaffin cells. Bovine chromaffin cells were isolated from fresh bovine adrenal glands by perfusion with collagenase, purified on self-generating Percoll gradients and maintained in culture as previously described (Thahouly et al., 2021). To induce exocytosis, intact chromaffin cells were washed twice with Locke's solution (140 mM NaCl, 4.7 mM KCl, 2.5 mM CaCl₂, 1.2 mM KH₂PO₄, 1.2 mM MgSO₄, 11 mM glucose, 0.56 mM ascorbic acid, 0.01 mM EDTA and 15 mM Hepes, pH 7.5), and then stimulated with Locke's solution containing 20 μ M nicotine or a 59 mM depolarizing K⁺ solution (85.7 mM NaCl, 59 mM KCl, 2.5 mM CaCl₂, 1.2 mM KH₂PO₄, 1.2 mM MgSO₄, 11 mM glucose, 0.56 mM ascorbic acid, 0.01 mM EDTA and 15 mM Hepes, pH 7.2). Mouse adrenal glands from 8 to 12-week-old males were dissected and chromaffin cells purified from papain-digested medulla. Cells were seeded on collagen-coated coverslips and maintained at 37 °C, 5% CO₂ for 24–48h before experiments as previously described (Houy et al., 2015).

Amperometry. Mice or bovine chromaffin cells were washed with ascorbic acid-free Locke's solution and processed for catecholamine release measurements by amperometry. Carbon-fiber electrode of 5 μ m diameter (ALA Scientific) was held at a potential of +650 mV compared with the reference electrode (Ag/AgCl) and approached closely to GFP expressing cells. Catecholamine's secretion was induced by 10 s pressure ejection of a 100 mM depolarizing K⁺ solution from a micropipette positioned at 10 μ m from the cell and recorded for 60 s. Amperometric recordings were performed with an AMU130 (Radiometer Analytical) amplifier, sampled at 5 kHz, and digitally low-passed filtered at 1 kHz. Analysis of amperometric recordings was done as previously described (Poëa-Guyon et al., 2013) with a macro (obtained from Dr. R. Borges laboratory; <http://webpages.ull.es/users/rborges/>) written for Igor software (Wavemetrics), allowing automatic spike detection and extraction of spike parameters. The number of amperometric spikes was counted as the total number of spikes with an amplitude >5 pA within 60 s. The spike parameters analysis was restricted to spikes with amplitudes of at least 5 pA. Quantal size (Q) of individual spike is measured by calculating the spike area above the baseline.

Catecholamine and growth hormone (GH) secretion assays. Chromaffin cells maintained in 96-well plates (Thermo Fisher Scientific, France) were briefly washed twice with Locke's solution and processed as stated in the figure legends. Aliquots of the medium were collected at the end of each experiment and cells were lysed with 1% (v/v) Triton X-100 (Sigma, UK). Secretion using both set of samples was quantified using a fluorimetric assay for catecholamine content as previously described (Thahouly et al., 2021). Briefly, 20 μ l of sample were transferred to 96-well black-plates (Thermo Fisher Scientific, France), 150 μ l of CH₃COONa (1M, pH 6) and 15 μ l of K₃Fe (CN)₆ (0.25%) were added to each well to oxidize catecholamines to adrenochrome. Next 50 μ l of NaOH (5M) containing ascorbic acid (0.3 mg/ml) were added, to convert adrenochrome to adrenolutin (Gabel et al., 2019). The fluorescence emitted by adrenolutin (λ_{ex} : 430 nm, λ_{em} : 520 nm) was measured with a spectrofluorometer (LB940 Mithras, Berthold). Amounts released were expressed as a percentage of the total amount of catecholamine present in the cells. Plotted data are representative of at least three independent experiments, each carried out in triplicate. Transfection of bovine chromaffin cells expressing bicistronic vectors for siRNA targeting PLD1/2 and for GH expression was performed as described previously (Béglé et al., 2009). The efficiency of PLD1 silencing was established previously and endogenous PLD1 levels was reduced by more than 80% (Zenou-Meyer et al., 2007). GH secretion assays was described previously (de Barry et al., 2006). Total amount of GH present in cells prior to stimulation was not significantly different for the different conditions tested. Catecholamine levels from adrenal gland extracts were measured using the 3-CAT research Elisa kit from LDN (Eurobio, Les Ulis, France) according to the manufacturer's instructions.

Confocal microscopy. For immunocytochemistry, chromaffin cells, grown on fibronectin-coated glass coverslips, were fixed and labelled as described previously (Chasserot-Golaz et al., 1996). The transient accessibility of D β H to the plasma membrane of chromaffin cells was tested by incubating cells for 5 min in Locke's solution containing or not K⁺ 59 mM and anti-D β H antibodies diluted to 1:200. Labelled cells were visualized using a Leica SP5II confocal microscope with a 63X objective. To compare the labeling of cells from different conditions within the same experiment, images were acquired at equatorial plane of the nucleus with the same parameters of the lasers and photomultipliers. The amount of D β H labelling associated with the plasma membrane was measured with ICY software and expressed as arbitrary units (A.U.) per pixel.

PC12 cell culture. PC12 cells were cultured in 5% CO₂, in DMEM supplemented with 10% horse serum, 5% fetal bovine serum, penicillin (100 U/ml) and streptomycin (100 g/ml) as previously reported (Béglé et al., 2009). Cells were transfected using Lipofectamine 2000 (Invitrogen) according to manufacturer's protocol.

Spinning disk microscopy. PC12 cells expressing NPY-RFP were used to follow the secretory granule's dynamics. Z-stacks are recorded with a spinning disk confocal microscope (Zeiss Axio Observer Z1 with a Yokogawa CSU X1 confocal head and a 100X objective) every 630 ms during 1 min. 40 stacks of 0.3 μ m were piled to get 12 μ m depth series. Movies were analyzed using ICY software to detect NPY-RFP spots (plugin "Spot Detector"), follow granules trajectories (plugin "Spot Tracking") and extract motion parameters (plugin "Track Manager") of each track. Vesicles tracked for fewer than 50 frames (30 s) were excluded from the analysis. Mean velocity of granules (μ m/s) was quantified using the total distance covered in 30 s. To differentiate the 3 categories of granule motion, filtering was applied using the extent of the displacement (μ m), given by the largest distance covered by the granule in 30 s, and the mean squared displacement (MSD) fitting curve. Granules displaying a directed motion show an extent >2.5 μ m and increasing velocity over time.

D β H internalization assay. The assay was performed as previously described (Ceridono et al., 2011). Briefly, after stimulation, cells were incubated 1 hr with anti-D β H antibody at 4 °C in the presence or not of 750 nM 5-Fluoro-2-indolyl des-chlorhalopemide (FIFI). Cells were washed and replaced at 37 °C for the indicated amount of time before being fixed, permeabilized, and processed for immunofluorescence. The percentage of internalized vesicles resulting from compensatory endocytosis was estimated using the

Euclidian distance map method. Briefly, distance from the cell periphery was transformed into grey values and segmented spots corresponding to D β H staining were reported on the grey levels map with 0 value corresponding to the plasma membrane. Each spot with a value > 15 is considered as an internalized vesicle when $\times 63$ and 1.4NA objective is used.

Reagents, drawing, and statistics. FIPI, CAY93, CAY94 were purchased from Cayman Chemicals and dissolved in DMSO. Drawings in Figs. 3A, 5A and 6 were created using BioRender.com. Statistical significance has been assessed using SigmaPlot 13 and GraphPad Prism 9.2 software. In the figure legends, n represents the number of experiments or the number of cells analyzed as specified.

3. Results and discussion

Carbon fiber amperometry is a well-suited technique to assess single vesicle rate of exocytosis from cells secreting biological active monoamines including serotonin, dopamine, adrenaline and noradrenaline. Amperometric recordings of individual mouse chromaffin cells revealed a decrease of nearly 60% in the frequency of amperometric events corresponding to single granule fusion in *Pld1*^{-/-} knockout cells (Fig. 1A). In contrast, no differences were observed in chromaffin cells from *Pld2*^{-/-} knockout animals. Supporting these observations, GH secretion assays performed in bovine chromaffin cells silenced for PLD1 showed that GH release was inhibited to similar extent, whereas PLD2 silencing had no effect (Fig. 1B). The role of PLD1 in secretion was further substantiated using specific inhibitors in fluorescent catecholamine secretion assay. A PLD1 and PLD2 dual inhibitor (FIPI) and an isoform-selective PLD1 inhibitor (CAY93) reduced catecholamine secretion, whereas an isoform-selective PLD2 inhibitor had no effect. (Fig. 1C). The effects of the PLD inhibitors are quickly reversible as the presence of the inhibitors during the stimulation period is necessary to observe the full inhibitory effect. Indeed when cells are preincubated for 1 h with the inhibitors and stimulated in their absence, secretion was inhibited by only 10–20% (data not shown), clearly arguing for a very rapid reversibility of their effects on exocytosis. Of note, analysis of the individual spike parameters revealed no significant reduction in the quantal release from single secretory events recorded by amperometry from either mouse *Pld1*^{-/-} chromaffin cells or bovine chromaffin cells inhibited by FIPI or CAY93 (data not shown). Therefore genetic, silencing, and pharmacological approaches all support the notion that PLD1 enzymatic activity (i.e. hydrolysis of phosphatidylcholine (PC) into choline and PA) is required for efficient catecholamine release in chromaffin cells without affecting secretory granule loading in catecholamine. Compelling evidences support an essential role for PA in a variety of exocytotic events in different cell models and secretory systems (Bader and Vitale, 2009; Kanaho et al., 2013; Waselle et al., 2005). PA is also implicated in autophagy (Holland et al., 2016), phagocytosis (Corrotte et al., 2006; Tanguy et al., 2019a), intracellular pathways such as tubular endosome biogenesis (Giridharan et al., 2013), Golgi vesicle formation (Ktistakis et al., 1996), mitochondria dynamics (Adachi et al., 2016), membrane wound repair (Vaughan et al., 2014) and neurite outgrowth (Ammar et al., 2013a,b). However, despite or perhaps due to these wide involvements, precise functions of PA along the secretory pathway remain unclear. The diversity of PA biosynthetic routes together with the possible occurrence of many different PA species, based on their fatty acyl chain composition, open the possibility for multiple roles in a given cellular function.

To address whether decrease in catecholamine release observed in the absence of PLD1 could be the consequence of a dramatic

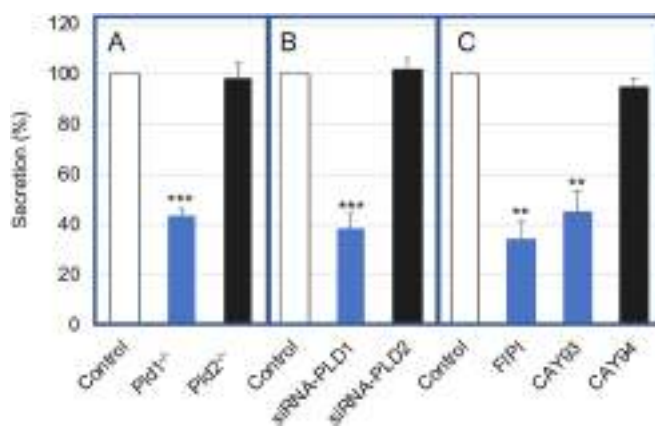


Fig. 1. Genetic, silencing and pharmacological alteration of PLD1 activity inhibited secretion from chromaffin cells. A) Mice chromaffin cells in culture were stimulated with a local application of 100 μ M of nicotine for 10 s and catecholamine secretion was monitored using carbon fiber amperometry. The number of spikes per cell from *Pld1*^{-/-} and *Pld2*^{-/-} mice was normalized to that of wild-type (Control). Data are given as the mean values \pm S.D. ($n > 75$ cells in each condition, *** $p < 0.001$ compared to control, one-way ANOVA). B) Bovine chromaffin cells co-expressing GH and siRNA for PLD1, PLD2, or a control siRNA were stimulated for 10 min with a K^+ 59 mM depolarizing solution and the percentage of GH secretion was normalized to that of the control condition. Data are given as the mean values \pm S.D. ($n = 4$ independent experiments, *** $p < 0.001$ compared to control, one-way ANOVA). C) Bovine chromaffin cells in culture were treated with the PLD inhibitors FIPI (750 nM), CAY93 (50 nM) or CAY94 (50 nM) for 1 h before stimulation for 10 min with 59 mM K^+ . Secretion of catecholamine was estimated using a fluorimetric assay by measuring catecholamine levels in supernatant and cell pellets. Secretion was normalized to control condition. Data are given as the mean values \pm S.D. obtained in three experiments performed on different cell cultures ($n = 3$, ** $p < 0.01$ compared to control, one-way ANOVA).

alteration of granule biogenesis and/or loading in catecholamine, we evaluated catecholamine levels in adrenal medulla and granule numbers in chromaffin cells obtained from wild-type and *Pld1*^{-/-} mouse. We found no significant differences in the total weight of adrenal glands or in total gland adrenaline and noradrenaline content for the two genotypes (Fig. 2A–C). We found, however, a significant reduction in the number and size of secretory granules in *Pld1*^{-/-} knockout mice (Fig. 2D and E). Nonetheless it is unlikely that these small reductions in granule number and diameter explain alone the potent inhibition of secretion. All these observations support the notion that PA produced by PLD1 moderately regulates granule biogenesis, but more strongly controls late stages of exocytosis in chromaffin cells. Incubation of chromaffin cells with an anti-DβH antibody allows for a direct visualization of exocytotic spots because the DβH epitope is exclusively exposed to the cell surface after secretory granule fusion with the plasma membrane (Fig. 3A). FIPI treatment reduced anti-DβH staining after stimulation of exocytosis by around 50% (Fig. 3B and C), confirming the notion that PLD activity is indeed required for effective exocytosis. More interestingly the inhibitory effect of FIPI on DβH staining was significantly rescued by provision in the culture medium of a mixture of PA or more specifically with a mono-unsaturated form of PA, PA(36:1) (Fig. 3C), suggesting that these forms of PA could modulate the amounts of exocytotic sites. It is also of note that provision of poly-unsaturated PA, PA(40:6) significantly increased DβH staining in resting condition (Fig. 3C), suggesting that this ω-3 form of PA favors fusion of already docked/primed granules without an increase of cytosolic calcium levels. All these observations are in line with our recent findings obtained by combining amperometry with electron microscopy of roof-top plasma membrane sheets which allowed us to propose that PLD1-generated PA has a composite role acting sequentially on granule docking and fusion (Tanguy et al., 2020). It is however notable that PA produced by PLD1, most likely at the level of the Golgi apparatus, plays a positive role in biogenesis. We recently reported evidence for a PA-binding domain in the granule-contained chromogranin A protein (Carmon et al., 2020), a well-appreciated granulogenic protein (Kim et al., 2001). This potential PA-chromogranin A interaction at the trans-Golgi network may thus contribute to membrane topology changes needed for granule biogenesis.

Before pre-mature secretory granules are actually docked at the plasma membrane, they need to be transported to the cell periphery (Tanguy et al., 2016). This active transport involves microtubules and motor proteins (Trifaró et al., 2008). To address whether PA might be required for secretory granule transport, we treated chromaffin cells with FIPI and explored the dynamics of secretory granule labelled with red fluorescent protein-fused neuropeptide Y (NPY-RFP) by spinning disk confocal microscopy (Fig. 4A). In agreement with previous observations (Maucourt et al., 2014), 3D imaging tracking and trajectory analysis indicated that most granules in the center of cells display random movements, whereas most granules found close to the plasma membrane have restricted movements. The first pool of granule likely corresponds to young newly formed pre-mature secretory granules, whereas the later population are probably mostly mature granules trapped in the dense cortical actin network and/or docked at exocytotic sites. A third population of NPY-RFP granules displays a directed movement generally from the center towards the cell periphery by what appears to be a conveyor

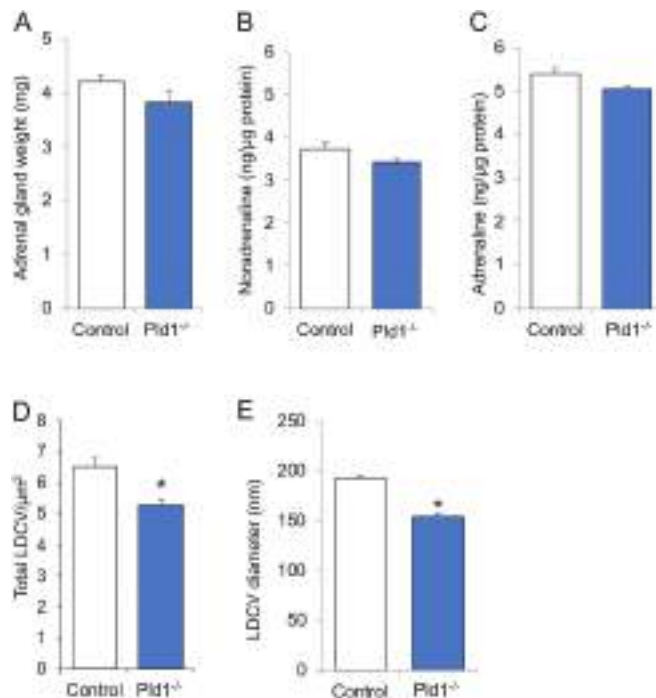


Fig. 2. Characterization of adrenal glands and chromaffin cells from PLD1^{-/-} mice. A) Adrenal glands were collected from wild-type (Control) and *Pld1*^{-/-} mice and weighted (n = 5). B,C) Noradrenaline and adrenaline levels from these glands were measured using the 3-CAT research Elisa kit (n = 5). A–C) Data are given as the mean values ± S.D. D) Quantification of the number of secretory granules (n = 6 mice per condition; 50 cells per mouse adrenal medulla). *p < 0.05, Mann-Whitney test). Means ± S.E.M. are plotted. E) Quantification of the dense core diameter of secretory granules (n = 6 mice per condition; 950 granules). *p < 0.05, Mann-Whitney test). Means ± S.E.M. are plotted.

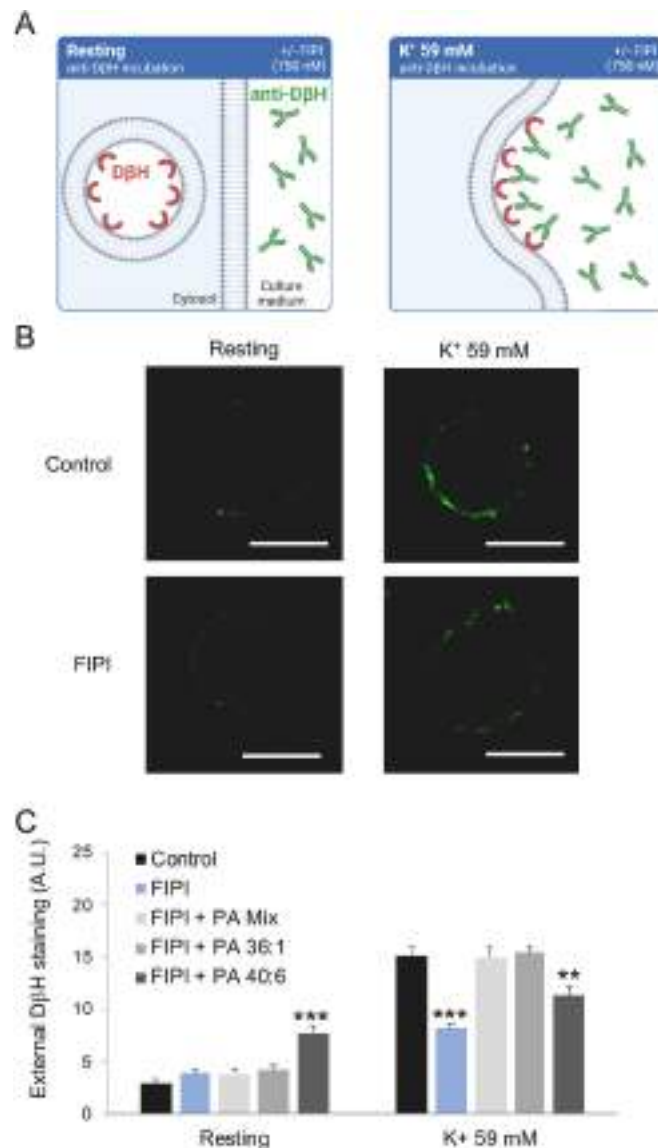


Fig. 3. Inhibition of PLD reduces the number of exocytosis spots at the plasma membrane. A) Schematic depiction of exocytotic spots imaging using DβH antibodies (anti-DβH). After stimulation of exocytosis with a depolarizing K⁺ solution and subsequent granule fusion with the plasma membrane, DβH becomes transiently accessible to anti-DβH antibodies added in the extracellular medium. B) Representative confocal pictures of extracellular DβH staining (green) at the plasma membrane. Bovine chromaffin cells preincubated for 1 h with FIPI 750 nM (FIPI) or DMSO 0.01% (Control) were maintained at rest (resting) or stimulated with 59 mM of K⁺ containing anti-DβH ± FIPI for 5 min, then fixed and processed for immunofluorescence. Bar = 10 μm. C) Quantification of extracellular DBH staining. Chromaffin cells were treated as in B, but also incubated with different PA species for 15 min prior to cell stimulation. Data are presented as means of fluorescence intensity per cell ± S.E.M (with 23 < n < 29 cells for each condition), obtained from three different cell cultures. **p < 0.01, ***p < 0.001 compared to control (Mann-Whitney Test).

belt mechanism. Analysis of total granule motion indicated that after FIPI treatment granules travel at lower speed (Fig. 4A and B). Then we focused on the three types of movements by filtering extent and velocity of tracks, extracting for instance a population of granules displaying a directed motion (Fig. 4C). Of note, we found that FIPI treatment significantly and specifically inhibited the mean squared displacement of granules harboring the typical directed movement (Fig. 4D). Intriguingly, inhibition of PLD did not affect the mean squared displacement of the “docked-like” population of granules (data not shown), which may require greater z-resolution through acquisition for instance using polarized TIRF microscopy (Anantharam et al., 2010). Hence these data are in favor of a model where PA produced by PLD also controls granule transport towards the exocytotic sites. An interesting study recently reported that binding to PA by the heavy chain of the motor protein kinesin-1 KIF5A is required for the vesicular association of the motor protein to MT1-MMP containing vesicles in lung cancer cells (Wang et al., 2017). We can thus postulate that the motor responsible for secretory granule movement along microtubules also requires binding to PA on secretory granules. Interestingly, we recently reported that

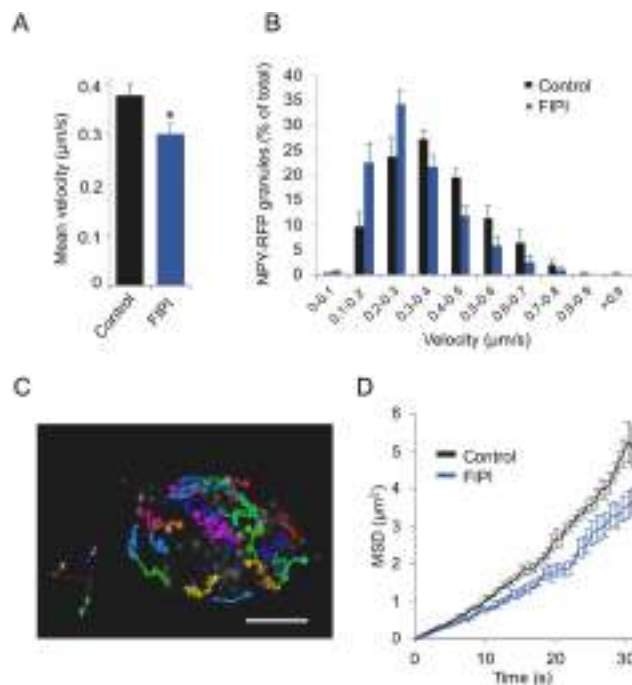


Fig. 4. PLD activity regulates mobility of secretory granules displaying a directed motion. A) Quantification of mean velocity of NPY-RFP granules. PC12 cells transiently expressing NPY-RFP (granular marker) were incubated 1 hr at 37 °C with FIPI or DMSO (Control). For each cell the motion of at least 150 granules was analyzed. Data are presented as means \pm S.E.M with $n = 9$ cells for each condition, obtained from three independent experiments. * $p < 0.05$ (Student *t*-test). B) Distribution of NPY-RFP granules in function of velocity (0.1 $\mu\text{m/s}$ intervals). Data are presented as means \pm S.E.M with $n = 9$ cells for each condition, obtained from three independent experiments. C) 3D visualization of tracks of granules displaying a directed motion in a cell transiently expressing NPY-RFP. After filtering by extent and velocity profile, granules displaying a directed motion were specifically analyzed. Bar = 5 μm . D) Mean squared displacement (MSD) of granules displaying a directed motion. Data are presented as means \pm S.E.M with $n = 9$ cells for each condition, obtained from three independent experiments. For each cell 10–20 tracks were analyzed and pooled. * $p < 0.05$ (one-way ANOVA).

purified secretory granules from PC12 cells have a high content in poly-unsaturated PA (Tanguy et al., 2020). This effect on granule movement was observed after 1 h of FIPI incubation, a period of time too short for a dramatic replacement of this population of granules, it is thus unlikely that it could be attributed to an action on PLD present in the Golgi. Although PLD isoenzymes were reported on secretory granules from various cell types (Freyberg et al., 2003), to our knowledge neither PLD1 nor PLD2 have been detected on purified chromaffin secretory granules and this even using mass spectrometry detection (Wegrzyn et al., 2010). Nevertheless, it is possible that yet undetectable amounts of PLD are associated with the chromaffin granule membrane and contribute to maintain the high levels of poly-unsaturated PA in these organelles. Those enzymes may thus regulate the binding or the activity of a motor kinesin protein that remains to be identified. An alternative explanation could also be linked to an indirect effect of inhibition of PLD at the plasma membrane on granule motility by directly impacting the cytoskeleton. Regarding this possibility, it is noteworthy that AnxA2 that regulates the formation of large actin bundles anchoring secretory granules to the plasma membrane (Gabel et al., 2015), also binds to PA (Gabel et al., 2019).

After exocytosis through full fusion also named full collapse, the secretory granule membrane is transiently incorporated in the plasma membrane. However, to maintain cell surface relatively constant, to preserve the specific lipid and protein composition of the plasma membrane, and finally to recycle the granular components, the secretory granule membrane is selectively recaptured. As for neurons, convincing evidence for this process named compensatory endocytosis have been also provided in chromaffin cells (Ceridono et al., 2011; Ory et al., 2013). A functional assay to monitor compensatory endocytosis relies on the use of a probe that would specifically label recycled constituents from the secretory granule membrane. Hence, we incubated chromaffin cells with an anti-D β H antibody which is internalized together with D β H upon chase and could be revealed with a secondary antibody after fixation and permeabilization of cells (Fig. 5A). After confocal images acquisition and Euclidian distance map analysis, we evaluated the internalization of these anti-D β H positive vesicular structures (Fig. 5B and C). We found that after 5 min of chase in control conditions nearly half of the anti-D β H positive vesicular structures were already internalized at distance from the plasma membrane. Of note FIPI treatment was applied immediately after cell stimulation and at 4 °C to prevent the inhibitory effect on exocytosis. On one hand, we observed a significant reduction in the proportion of internalized structures after 5 min of chase (Fig. 5C). On the other hand, after 30 min of chase FIPI treatment had no significant effect with nearly 60% of anti-D β H positive vesicular structures internalized both in the control and FIPI conditions. These observations are clearly in line with the proposed function of PA by diacylglycerol (DAG) kinase (DGK) in synaptic vesicle cycle (Tu-Sekine et al., 2015), but clearly suggest that probing the contribution of DGK in secretory granule

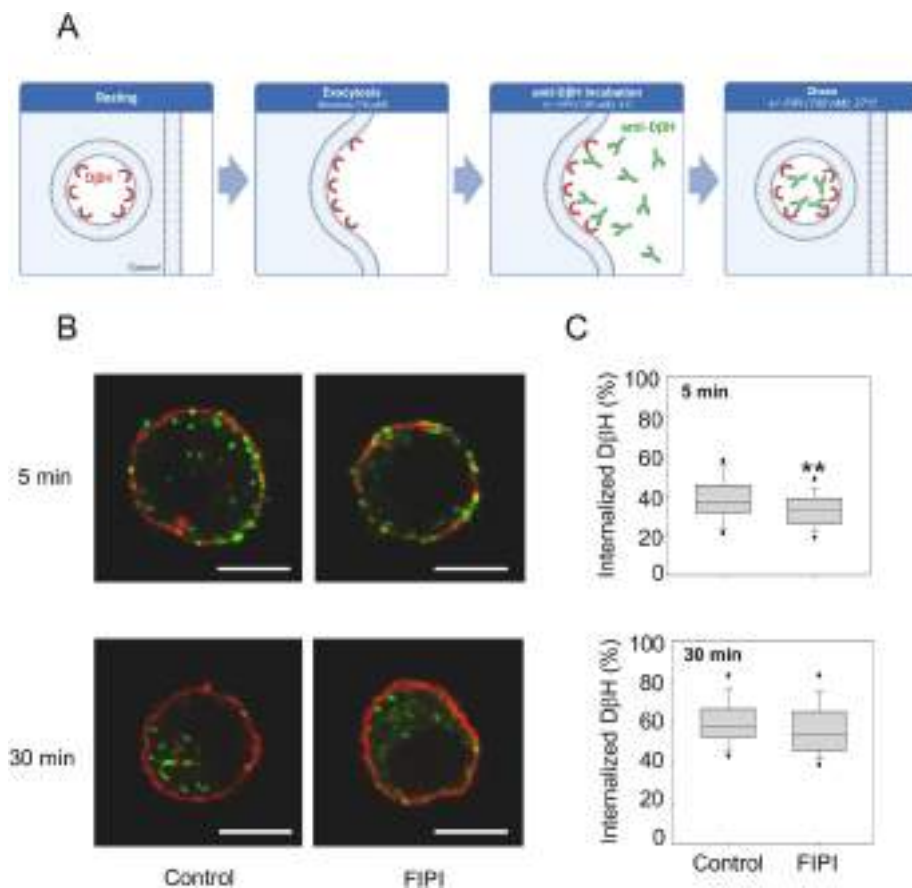


Fig. 5. Inhibition of PLD after exocytosis slows down compensatory endocytosis. A) Schematic depiction of anti-DβH antibodies internalization assay. B) Representative confocal pictures of DβH staining (green) and cortical F-actin staining (red). Chromaffin cells were stimulated with nicotine 10 μM during 10 min. After a short rinse, cells are incubated for 1 h at 4 °C with Locke solution containing anti-DβH antibodies and FIPI 750 nM (FIPI) or DMSO 0.01% (Control). Cells are then incubated at 37 °C during 5 or 30 min to trigger anti-DβH antibodies internalization, fixed and processed for immunofluorescence. Bar = 10 μm. C) Quantification of the percentage of internalized vesicles after 5 or 30 min of compensatory endocytosis, using the Euclidian distance map method. Data are presented as box-and-whisker plots (depicting median as black line and mean as white line), with 56 < n < 61 cells for each condition, obtained from four different cell cultures. **p < 0.01 compared to control (Mann-Whitney Test).

endocytosis remains to be evaluated. Altogether these results indicate that PA generated by PLD, but also potentially by other sources also contributes to optimal compensatory endocytosis, but our chase analysis suggest that the contribution of PA produced by PLD most likely occurs only during the early stages of compensatory endocytosis.

Incubation of cultured chromaffin cells with PA micelles proved to be an effective approach to identify the PA species able to compensate for the lack of PLD activity at the plasma membrane of PLD1-depleted cells. Indeed, exogenous PA reached the intracellular leaflet of the plasma membrane within minutes as seen using the PA sensor Spo20p-GFP which was recruited to the cell membrane shortly after addition of PA micelles to cell culture medium (Tanguy et al., 2020). Incubation of chromaffin cells with a mixture of various forms of PA did not significantly affect catecholamine secretion *per se* in cells fully capable to produce this lipid. However, it rescued secretion from cells treated with PLD inhibitors. Interestingly, mono- and di-unsaturated forms of PA rescued secretion levels in PLD1-depleted cells back to levels of untreated cells, whereas poly-unsaturated PA did not. Using a combination of amperometric recordings and ultrastructural observations on plasma membrane sheets, we observed that mono- and di-unsaturated forms of PA are apparently involved in granule recruitment and/or docking thereby controlling the number of exocytotic events. In contrast, poly-unsaturated ω3 PA seem to be specifically implicated in fusion pore dilation (Fig. 6). At present, it is not known if optimal secretory vesicle biogenesis, transport and compensatory endocytosis require specific species of PA (Fig. 6), but clearly tackling this aspect represents the next step to better understand the fine tuning of the numerous steps along the secretory pathway by different forms of PA.

Understanding the input of other potential contributors of PA synthesis such as DGK and lysophosphatidic acid-acyltransferases will also be important, especially since these enzymes have also been reported to contribute to the exo-endocytosis cycle of synaptic vesicles (Barber and Raben, 2020; Schwarz et al., 2011). On the same line, the future of newly synthesized PA during exocytosis remains to be clarified. As exocytosis is highly regulated, it is anticipated that PA levels of the specialized exocytosis sites rapidly

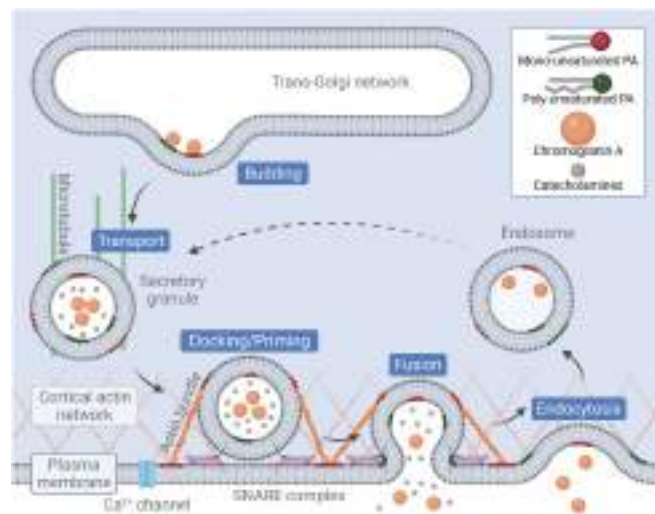


Fig. 6. Model depicting the different steps along the secretory process regulated by PA.

PA modulates secretory granule biogenesis, transport, docking, fusion and compensatory endocytosis along the secretory pathway. Mono-unsaturated PA is specifically involved in granule docking and poly-unsaturated PA acts on fusion pore dynamics. Dotted arrow indicates potential recycling of endocytosed components to secretory granules that remains to be firmly established experimentally.

decrease after exocytosis is halted. The use of PA sensors revealed apparent high levels of PA at the plasma membrane remaining for several minutes after secretion ending in chromaffin cells (Zeniou-Meyer et al., 2007). But this might not actually reflect the correct metabolism of PA as those sensors most likely compete with the endogenous enzymes involved in PA metabolism and thus artificially prevent its degradation. Among these enzymes involved in PA metabolism there are phospholipase A1 (PLA1) and PLA2 that, respectively, cleave the ester bridge of the glycerol backbone of PA in *sn*1 and *sn*2 positions, producing lyso-PA and free fatty acids (Tanguy et al., 2018). Note that PLA1 activity mostly generates saturated fatty acids whereas unsaturated fatty acids are produced by PLA2. A third class of enzyme called PA-phosphatase or lipins can transform PA into DAG (Tanguy et al., 2018). Overexpression of lipin-1 into chromaffin cells inhibited exocytosis measured by amperometry validating the concept that PA degradation might represent a stop signal for exocytosis (Baneux et al., 2020). However, partial reduction of endogenous level of lipins by RNA interference did not significantly modify the secretory activity of PC12 cells (Baneux et al., 2020), indicating that either the silencing was not effective enough or that enzymes of the phospholipases A family are the major contributor of PA metabolism to terminate the PA exocytosis signal. Furthermore, the eventual transport of PA to other organelles, such as the endoplasmic reticulum, through membrane contact sites cannot be excluded either. Those structures which have been identified recently (Nishimura and Stefan, 2020) could not only answer the question of PA elimination from active exocytosis sites but also offer fascinating perspectives regarding the recycling of PA into PC.

Finally, the molecular mechanisms by which PA is playing so many related, yet different functions along the secretory pathway is another fundamental question that remains largely unanswered. Intriguingly PC to PA conversion by PLD transforms a cylindrical phospholipid into a conical one. Since biophysical models have proposed that intermediates of the membrane fusion reaction require such cone- or inverted cone-shaped lipids, a direct role of PA as a fusogenic lipid has been proposed (Vitale et al., 2001). Two possibilities to explain the differential effects of mono- and poly-unsaturated PA species on exocytosis is that they adopt different geometry and might thus differently affect membrane topology (Chernomordik et al., 1995) or recruit different effectors involved specifically in vesicle docking or fusion. Among the nearly 50 different proteins that have been shown to date to bind to PA (Pokotylo et al., 2018; Tanguy et al., 2019b; Zegarlińska et al., 2018), their ability to interact with specific forms of PA has not been extensively evaluated, but some information on these aspects are starting to emerge. Using an *in vitro* fluorescence liposome-based assay, we recently found that the PA-binding domain of Spo20p, Opi1p, and PDE4A1 proteins are partially sensitive to the fatty acyl length and saturation, displaying a clear preference for mono- and poly-unsaturated PA over saturated PA (Kassas et al., 2017). Of interest a clear specificity for poly-unsaturated PA was also recently described for L-lactate dehydrogenase A, which affected enzymatic activity (Hoshino and Sakane, 2020). Among the many potential PA interactors involved along the secretory pathway (Tanguy et al., 2018), we can cite a few. For instance, the granulogenic protein chromogranin A was recently reported to bind PA *in vitro* and these two partners might act together to favor membrane deformation at the TGN and granule biogenesis (Carmon et al., 2020). PA in the secretory granule membrane could also regulate the binding of a kinesin or its processing activity as reported for MT1-MMP containing vesicles in lung cancer cells (Wang et al., 2017). The SNARE protein syntaxin-1 is one of the first target candidate that comes in mind as a target protein in the secretory machinery, as it has been shown to bind to several anionic lipids including PI and PA (Lam et al., 2008). Indeed suppression of its polybasic site abolished the ability of syntaxin-1 to bind PA and resulted in a reduction of the number of amperometric spikes and increased delay of the fusion pore expansion in PC12 cells (Lam et al., 2008), very similarly to the amperometric traces obtained in *Pld1*^{-/-} mice chromaffin cells or in bovine chromaffin cells with pharmacologically inhibited PLD1 activity (Tanguy

et al., 2020). The next challenge will be to determine if the functions of these regulators in the exocytotic machinery involves their ability to bind PA and whether they require a partnership with specific PA species.

CRedit authorship contribution statement

Emeline Tanguy: Formal analysis, planned and carried out experimental work and analyzed results. **Alexander Wolf:** Formal analysis, planned and carried out experimental work and analyzed results. Draw parts of figures. **Qili Wang:** Formal analysis, planned and carried out experimental work and analyzed results. **Sylvette Chasserot-Golaz:** Methodology, contributed to methodology. **Stéphane Ory:** Methodology, contributed to methodology. **Stéphane Gasman:** Funding acquisition, supervision. **Nicolas Vitale:** Funding acquisition, supervision, writing original draft and editing. All authors contributed and agreed to the final version of the manuscript.

Declaration of competing interest

The authors declare that they have no known competing financial interests or personal relationships that could have appeared to influence the work reported in this paper.

Acknowledgment

We acknowledge the In Vitro Imaging Platform of ITI Neurostra at CNRS UAR-3256, Dr. Jean-Daniel Fauny at the Imaging Platform of IBMC (CNRS UPR-3572, Strasbourg) for technical assistance with spinning disk confocal microscopy, the municipal slaughterhouse of Haguenau (France) for providing the bovine adrenal glands, and the INCI animal facility for handling mice.

E.T. was supported by grant from INSERM (Fondation Bettencourt Schueller). This work was supported by grants from the Fondation pour la Recherche Médicale (DEI20151234424) and the Agence Nationale pour la Recherche (ANR-19-CE44-0019) to N.V. INSERM is providing the salary to SCG, SG and NV.

Abbreviations

DAG	Diacylglycerol
FIPI	5-Fluoro-2-indolyl des-chlorohalopemide
GH	Growth hormone
NPY-RFP	Neuropeptide Y fused to red fluorescent protein
PA	Phosphatidic acid
PC	Phosphatidylcholine
PI	Phosphoinositide
PLA	Phospholipase A
PLD	Phospholipase D

References

- Adachi, Y., Itoh, K., Yamada, T., Cervený, K.L., Suzuki, T.L., Macdonald, P., Frohman, M.A., Ramachandran, R., Iijima, M., Sesaki, H., 2016. Coincident phosphatidic acid interaction restrains Drp1 in mitochondrial division. *Mol. Cell* 63, 1034–1043. <https://doi.org/10.1016/j.molcel.2016.08.013>.
- Ammar, M.-R., Humeau, Y., Hanauer, A., Nieswandt, B., Bader, M.-F., Vitale, N., 2013a. The coffin-lowry syndrome-associated protein RSK2 regulates neurite outgrowth through phosphorylation of phospholipase D1 (PLD1) and synthesis of phosphatidic acid. *J. Neurosci.* 33, 19470–19479. <https://doi.org/10.1523/JNEUROSCI.2283-13.2013>.
- Ammar, M.R., Kassas, N., Chasserot-Golaz, S., Bader, M.-F., Vitale, N., 2013b. Lipids in regulated exocytosis: what are they doing? *Front. Endocrinol.* 4, 125. <https://doi.org/10.3389/fendo.2013.00125>.
- Ammar, M.R., Thahouly, T., Hanauer, A., Stegner, D., Nieswandt, B., Vitale, N., 2015. PLD1 participates in BDNF-induced signalling in cortical neurons. *Sci. Rep.* 5, 14778. <https://doi.org/10.1038/srep14778>.
- Anantharam, A., Onoa, B., Edwards, R.H., Holz, R.W., Axelrod, D., 2010. Localized topological changes of the plasma membrane upon exocytosis visualized by polarized TIRFM. *J. Cell Biol.* 188 (3), 415–428. <https://doi.org/10.1083/jcb.200908010>.
- Bader, M.-F., Vitale, N., 2009. Phospholipase D in calcium-regulated exocytosis: lessons from chromaffin cells. *Biochim. Biophys. Acta* 1791, 936–941. <https://doi.org/10.1016/j.bbalip.2009.02.016>.
- Baneux, C., Tanguy, E., Thahouly, T., Vitale, A., Chasserot-Golaz, S., Bader, M.-F., Gasman, S., Vitale, N., 2020. Phosphatidic acid metabolism regulates neuroendocrine secretion but is not under the direct control of lipins. *IUBMB Life* 72, 533–543. <https://doi.org/10.1002/iub.2229>.
- Barber, C.N., Raben, D.M., 2020. Roles of DGKs in neurons: postsynaptic functions? *Advances in biological regulation. Symposium issue 2019* 75, 100688. <https://doi.org/10.1016/j.jbior.2019.100688>.
- Béglé, A., Tryoen-Tóth, P., de Barry, J., Bader, M.-F., Vitale, N., 2009. ARF6 regulates the synthesis of fusogenic lipids for calcium-regulated exocytosis in neuroendocrine cells. *J. Biol. Chem.* 284, 4836–4845. <https://doi.org/10.1074/jbc.M806894200>.
- Bigay, J., Antonny, B., 2012. Curvature, lipid packing, and electrostatics of membrane organelles: defining cellular territories in determining specificity. *Dev. Cell* 23, 886–895. <https://doi.org/10.1016/j.devcel.2012.10.009>.
- Bowling, F.Z., Frohman, M.A., Airola, M.V., 2021. Structure and function of human phospholipase D. *Adv. Biol. Regul.* 79, 100783. <https://doi.org/10.1016/j.jbior.2020.100783>.

- Bullen, H.E., Bisio, H., Soldati-Favre, D., 2019. The triumvirate of signaling molecules controlling *Toxoplasma* microneme exocytosis: cyclic GMP, calcium, and phosphatidic acid. *PLoS Pathog.* 15 (5), e1007670 <https://doi.org/10.1371/journal.ppat.1007670>.
- Burgess, T.L., Kelly, R.B., 1987. Constitutive and regulated secretion of proteins. *Annu. Rev. Cell Biol.* 3, 243–293. <https://doi.org/10.1146/annurev.cb.03.110187.001331>.
- Carmon, O., Laguerre, F., Riachy, L., Delestre-Delacour, C., Wang, Q., Tanguy, E., Jeandel, L., Cartier, D., Thahouly, T., Haeberlé, A.-M., Fouillen, L., Rezaei, O., Schapman, D., Haefel, A., Goumon, Y., Galas, L., Renard, P.-Y., Alexandre, S., Vitale, N., Anouar, Y., Montero-Hadjadje, M., 2020. Chromogranin A preferential interaction with Golgi phosphatidic acid induces membrane deformation and contributes to secretory granule biogenesis. *FASEB J.: Off. Publ. Fed. Am. Soc. Exp. Biol.* 34, 6769–6790. <https://doi.org/10.1096/fj.202000074R>.
- Caumont, A.S., Galas, M.C., Vitale, N., Aunis, D., Bader, M.F., 1998. Regulated exocytosis in chromaffin cells. Translocation of ARF6 stimulates a plasma membrane-associated phospholipase D. *J. Biol. Chem.* 273, 1373–1379. <https://doi.org/10.1074/jbc.273.3.1373>.
- Ceridono, M., Ory, S., Momboise, F., Chasserot-Golaz, S., Houy, S., Calco, V., Haeberlé, A.-M., Demais, V., Bailly, Y., Bader, M.-F., Gasman, S., 2011. Selective recapture of secretory granule components after full collapse exocytosis in neuroendocrine chromaffin cells. *Traffic* 12, 72–88. <https://doi.org/10.1111/j.1600-0854.2010.01125.x>.
- Chasserot-Golaz, S., Vitale, N., Sagot, I., Delouche, B., Dirrig, S., Pradel, L.A., Henry, J.P., Aunis, D., Bader, M.F., 1996. Annexin II in exocytosis: catecholamine secretion requires the translocation of p36 to the subplasmalemmal region in chromaffin cells. *J. Cell Biol.* 133, 1217–1236. <https://doi.org/10.1083/jcb.133.6.1217>.
- Chernomordik, L., Chanturiya, A., Green, J., Zimmerberg, J., 1995. The hemifusion intermediate and its conversion to complete fusion: regulation by membrane composition. *Biophys. J.* 69, 922–929. [https://doi.org/10.1016/S0006-3495\(95\)79966-0](https://doi.org/10.1016/S0006-3495(95)79966-0).
- Choi, W.S., Kim, Y.M., Combs, C., Frohman, M.A., Beaven, M.A., 2002. Phospholipases D1 and D2 regulate different phases of exocytosis in mast cells. *J. Immunol.* 168, 5682–5689. <https://doi.org/10.4049/jimmunol.168.11.5682>.
- Corrotte, M., Chasserot-Golaz, S., Huang, P., Du, G., Ktistakis, N.T., Frohman, M.A., Vitale, N., Bader, M.-F., Grant, N.J., 2006. Dynamics and function of phospholipase D and phosphatidic acid during phagocytosis. *Traffic* 7, 365–377. <https://doi.org/10.1111/j.1600-0854.2006.00389.x>.
- de Barry, J., Janoshazi, A., Dupont, J.L., Proksch, O., Chasserot-Golaz, S., Jeromin, A., Vitale, N., 2006. Functional implication of neuronal calcium sensor-1 and phosphoinositide 4-kinase-beta interaction in regulated exocytosis of PC12 cells. *J. Biol. Chem.* 281, 18098–18111. <https://doi.org/10.1074/jbc.M509842200>.
- Freyberg, Z., Siddhanta, A., Shields, D., 2003. “Slip, sliding away”: phospholipase D and the Golgi apparatus. *Trends Cell Biol.* 13, 540–546. <https://doi.org/10.1016/j.tcb.2003.08.004>.
- Frohman, M.A., 2015. The phospholipase D superfamily as therapeutic targets. *Trends Pharmacol. Sci.* 36, 137–144. <https://doi.org/10.1016/j.tips.2015.01.001>.
- Gabel, M., Delavoie, F., Demais, V., Royer, C., Bailly, Y., Vitale, N., Bader, M.-F., Chasserot-Golaz, S., 2015. Annexin A2-dependent actin bundling promotes secretory granule docking to the plasma membrane and exocytosis. *J. Cell Biol.* 210, 785–800. <https://doi.org/10.1083/jcb.201412030>.
- Gabel, M., Delavoie, F., Royer, C., Thahouly, T., Gasman, S., Bader, M.-F., Vitale, N., Chasserot-Golaz, S., 2019. Phosphorylation cycling of Annexin A2 Tyr23 is critical for calcium-regulated exocytosis in neuroendocrine cells. *Biochimica Et Biophysica Acta. Mol. Cell Res.* 1866, 1207–1217. <https://doi.org/10.1016/j.bbamer.2018.12.013>.
- Galas, M.-C., Helms, J.B., Vitale, N., Thiersé, D., Aunis, D., Bader, M.-F., 1997. Regulated exocytosis in chromaffin cells A potential role for A secretory GRANULE-ASSOCIATED ARF6 protein. *J. Biol. Chem.* 272, 2788–2793. <https://doi.org/10.1074/jbc.272.5.2788>.
- Gasman, S., Vitale, N., 2017. Lipid remodelling in neuroendocrine secretion. *Biol. Cell.* 109, 381–390. <https://doi.org/10.1111/boc.201700030>.
- Giridharan, S.S.P., Cai, B., Vitale, N., Naslavsky, N., Caplan, S., 2013. Cooperation of MICAL-1, syndapin2, and phosphatidic acid in tubular recycling endosome biogenesis. *Mol. Biol. Cell* 24 (1776–1790), S1–S15. <https://doi.org/10.1091/mbc.E13-01-0026>.
- Holden, N.J., Savage, C.O., Young, S.P., Wakelam, M.J., Harper, L., Williams, J.M., 2011. A dual role for diacylglycerol kinase generated phosphatidic acid in autoantibody-induced neutrophil exocytosis. *Mol. Med.* 17 (11–12), 1242–1252. <https://doi.org/10.2119/molmed.2011.00028>, 2011.
- Holland, P., Knævelsrud, H., Søren, K., Mathai, B.J., Lystad, A.H., Pankiv, S., Bjørndal, G.T., Schultz, S.W., Lobert, V.H., Chan, R.B., Zhou, B., Liestøl, K., Carlsson, S. R., Melia, T.J., Di Paolo, G., Simonsen, A., 2016. HSBP3 negatively regulates autophagy by modulation of phosphatidic acid levels. *Nat. Commun.* 7, 13889. <https://doi.org/10.1038/ncomms13889>.
- Holthuis, J.C.M., Menon, A.K., 2014. Lipid landscapes and pipelines in membrane homeostasis. *Nature* 510, 48–57. <https://doi.org/10.1038/nature13474>.
- Hoshino, F., Sakane, F., 2020. Polyunsaturated fatty acid-containing phosphatidic acids selectively interact with L-lactate dehydrogenase A and induce its secondary structural change and inactivation. *Biochim. Biophys. Acta Mol. Cell Biol. Lipids* 1865, 158768. <https://doi.org/10.1016/j.bbalip.2020.158768>.
- Houy, S., Estay-Ahumada, C., Croisé, P., Calco, V., Haeberlé, A.-M., Bailly, Y., Billuart, P., Vitale, N., Bader, M.-F., Ory, S., Gasman, S., 2015. Oligophrenin-1 connects exocytotic fusion to compensatory endocytosis in neuroendocrine cells. *J. Neurosci.: Off. J. Soc. Neurosci.* 35, 11045–11055. <https://doi.org/10.1523/JNEUROSCI.4048-14.2015>.
- Hughes, W.E., Elgundi, Z., Huang, P., Frohman, M.A., Biden, T.J., 2004. Phospholipase D1 regulates secretagogue-stimulated insulin release in pancreatic beta-cells. *J. Biol. Chem.* 279, 27534–27541. <https://doi.org/10.1074/jbc.M403012200>.
- Jenkins, G.M., Frohman, M.A., 2005. Phospholipase D: a lipid centric review. *Cell. Mol. Life Sci.: CMLS* 62, 2305–2316. <https://doi.org/10.1007/s00018-005-5195-z>.
- Kanaho, Y., Sato, T., Hongu, T., Funakoshi, Y., 2013. Molecular mechanisms of fMLP-induced superoxide generation and degranulation in mouse neutrophils. *Adv. Biol. Regul.* 53 (1), 128–134. <https://doi.org/10.1016/j.jbior.2012.09.001>.
- Kassas, N., Tanguy, E., Thahouly, T., Fouillen, L., Heintz, D., Chasserot-Golaz, S., Bader, M.-F., Grant, N.J., Vitale, N., 2017. Comparative characterization of phosphatidic acid sensors and their localization during frustrated phagocytosis. *J. Biol. Chem.* 292, 4266–4279. <https://doi.org/10.1074/jbc.M116.742346>.
- Katan, M., Cockcroft, S., 2020. Phosphatidylinositol(4,5)bisphosphate: diverse functions at the plasma membrane. *Essays Biochem.* 64, 513–531. <https://doi.org/10.1042/EBC20200041>.
- Kim, S.-C., Wang, X., 2020. Phosphatidic acid: an emerging versatile class of cellular mediators. *Essays Biochem.* 64, 533–546. <https://doi.org/10.1042/EBC20190089>.
- Kim, T., Tao-Cheng, J.H., Eiden, L.E., Loh, Y.P., 2001. Chromogranin A, an “on/off” switch controlling dense-core secretory granule biogenesis. *Cell* 106, 499–509. [https://doi.org/10.1016/S0092-8674\(01\)00459-7](https://doi.org/10.1016/S0092-8674(01)00459-7).
- Kooijman, E.E., Chupin, V., Fuller, N.L., Kozlov, M.M., de Kruijff, B., Burger, K.N.J., Rand, P.R., 2005. Spontaneous curvature of phosphatidic acid and lysophosphatidic acid. *Biochemistry* 44, 2097–2102. <https://doi.org/10.1021/bi0478502>.
- Ktistakis, N.T., Brown, H.A., Waters, M.G., Sternweis, P.C., Roth, M.G., 1996. Evidence that phospholipase D mediates ADP ribosylation factor-dependent formation of Golgi coated vesicles. *J. Cell Biol.* 134, 295–306. <https://doi.org/10.1083/jcb.134.2.295>.
- Lam, A.D., Tryoen-Toth, P., Tsai, B., Vitale, N., Stuenkel, E.L., 2008. SNARE-catalyzed fusion events are regulated by Syntaxin1A-lipid interactions. *Mol. Biol. Cell* 19, 485–497. <https://doi.org/10.1091/mbc.e07-02-0148>.
- Marchini-Alves, C.M., Barbosa Lorenzi, V.C., da Silva, E.Z., Mazucato, V.M., Jamur, M.C., Oliver, C., 2015. Phospholipase D2 modulates the secretory pathway in RBL-2H3 mast cells. *PLoS One* 10 (10), e0139888. <https://doi.org/10.1371/journal.pone.0139888>, 2015 Oct 22.
- Maucourt, G., Kasula, R., Papadopoulos, A., Nieminen, T.A., Rubinstein-Dunlop, H., Meunier, F.A., 2014. Mapping organelle motion reveals a vesicular conveyor belt spatially replenishing secretory vesicles in stimulated chromaffin cells. *PLoS One* 9, e87242. <https://doi.org/10.1371/journal.pone.0087242>.
- Mima, J., Wickner, W., 2009. Complex lipid requirements for SNARE- and SNARE chaperone-dependent membrane fusion. *J. Biol. Chem.* 284, 27114–27122. <https://doi.org/10.1074/jbc.M109.010223>.
- Nishimura, T., Stefan, C.J., 2020. Specialized ER membrane domains for lipid metabolism and transport. *Biochimica et Biophysica Acta (BBA) - Molecular and Cell Biology of Lipids, Endoplasmic reticulum platforms for lipid dynamics* 1865, 158492. <https://doi.org/10.1016/j.bbalip.2019.07.001>.
- O’Lunaigh, N., Pardo, R., Fensome, A., Allen-Baume, V., Jones, D., Holt, M.R., Cockcroft, S., 2002. Continual production of phosphatidic acid by phospholipase D is essential for antigen-stimulated membrane ruffling in cultured mast cells. *MBoC* 13, 3730–3746. <https://doi.org/10.1091/mbc.e02-04-0213>.

- Ory, S., Ceridono, M., Momboise, F., Houy, S., Chasserot-Golaz, S., Heintz, D., Calco, V., Haeberlé, A.-M., Espinoza, F.A., Sims, P.J., Bailly, Y., Bader, M.-F., Gasman, S., 2013. Phospholipid scramblase-1-induced lipid reorganization regulates compensatory endocytosis in neuroendocrine cells. *J. Neurosci.* 33, 3545–3556. <https://doi.org/10.1523/JNEUROSCI.3654-12.2013>.
- Poëa-Guyon, S., Ammar, M.R., Erard, M., Amar, M., Moreau, A.W., Fossier, P., Gleize, V., Vitale, N., Morel, N., 2013. The V-ATPase membrane domain is a sensor of granular pH that controls the exocytotic machinery. *J. Cell Biol.* 203, 283–298. <https://doi.org/10.1083/jcb.201303104>.
- Pokotylo, I., Kravets, V., Martinec, J., Ruelland, E., 2018. The phosphatidic acid paradox: too many actions for one molecule class? Lessons from plants. *Prog. Lipid Res.* 71, 43–53. <https://doi.org/10.1016/j.plipres.2018.05.003>.
- Rizo, J., Xu, J., 2015. The synaptic vesicle release machinery. *Annu. Rev. Biophys.* 44, 339–367. <https://doi.org/10.1146/annurev-biophys-060414-034057>.
- Schwarz, K., Natarajan, S., Kassas, N., Vitale, N., Schmitz, F., 2011. The synaptic ribbon is a site of phosphatidic acid generation in ribbon synapses. *J. Neurosci.: Off. J. Soc. Neurosci.* 31, 15996–16011. <https://doi.org/10.1523/JNEUROSCI.2965-11.2011>.
- Tanguy, E., Carmon, O., Wang, Q., Jeandel, L., Chasserot-Golaz, S., Montero-Hadjadje, M., Vitale, N., 2016. Lipids implicated in the journey of a secretory granule: from biogenesis to fusion. *J. Neurochem.* 137, 904–912. <https://doi.org/10.1111/jnc.13577>.
- Tanguy, E., Costé de Bagneaux, P., Kassas, N., Ammar, M.-R., Wang, Q., Haeberlé, A.-M., Raherindratsara, J., Fouillen, L., Renard, P.-Y., Montero-Hadjadje, M., Chasserot-Golaz, S., Ory, S., Gasman, S., Bader, M.-F., Vitale, N., 2020. Mono- and poly-unsaturated phosphatidic acid regulate distinct steps of regulated exocytosis in neuroendocrine cells. *Cell Rep.* 32, 108026. <https://doi.org/10.1016/j.celrep.2020.108026>.
- Tanguy, E., Kassas, N., Vitale, N., 2018. Protein Phospholipid interaction motifs: a focus on phosphatidic acid. *Biomolecules* 8. <https://doi.org/10.3390/biom8020020>.
- Tanguy, E., Thahouly, T., Royer, C., Demais, V., Gasman, S., Chasserot-Golaz, S., Vitale, N., 2021. Protocol for electron microscopy ultrastructural localization of the fusogenic lipid phosphatidic acid on plasma membrane sheets from chromaffin cells. *STAR Protoc* 2, 100464. <https://doi.org/10.1016/j.xpro.2021.100464>.
- Tanguy, E., Tran Nguyen, A.P., Kassas, N., Bader, M.-F., Grant, N.J., Vitale, N., 2019a. Regulation of phospholipase D by Arf6 during FcγR-mediated phagocytosis. *J. Immunol.* 202, 2971–2981. <https://doi.org/10.4049/jimmunol.1801019>.
- Tanguy, E., Wang, Q., Moine, H., Vitale, N., 2019b. Phosphatidic acid: from pleiotropic functions to neuronal pathology. *Front. Cell. Neurosci.* 13, 2. <https://doi.org/10.3389/fncel.2019.00002>.
- Thahouly, T., Tanguy, E., Raherindratsara, J., Bader, M.-F., Chasserot-Golaz, S., Gasman, S., Vitale, N., 2021. Bovine chromaffin cells: culture and fluorescence assay for secretion. *Methods Mol. Biol.* 2233, 169–179. https://doi.org/10.1007/978-1-0716-1044-2_11.
- Trifaró, J.-M., Gasman, S., Gutiérrez, L.M., 2008. Cytoskeletal control of vesicle transport and exocytosis in chromaffin cells. *Acta Physiol.* 192, 165–172. <https://doi.org/10.1111/j.1748-1716.2007.01808.x>.
- Tu-Sekine, B., Goldschmidt, H., Raben, D.M., 2015. Diacylglycerol, phosphatidic acid, and their metabolic enzymes in synaptic vesicle recycling. *Adv. Biol. Regul.* 57, 147–152. <https://doi.org/10.1016/j.jbior.2014.09.010>.
- Vaughan, E.M., You, J.-S., Elsie Yu, H.-Y., Lasek, A., Vitale, N., Hornberger, T.A., Bement, W.M., 2014. Lipid domain-dependent regulation of single-cell wound repair. *Mol. Biol. Cell* 25, 1867–1876. <https://doi.org/10.1091/mbc.E14-03-0839>.
- Vázquez-Martínez, R., Díaz-Ruiz, A., Almabouada, F., Rabanal-Ruiz, Y., Gracia-Navarro, F., Malagón, M.M., 2012. Revisiting the regulated secretory pathway: from frogs to human. *Gen. Comp. Endocrinol.* 175, 1–9. <https://doi.org/10.1016/j.ygcen.2011.08.017>.
- Verhage, M., Sørensen, J.B., 2020. SNAREopathies: diversity in mechanisms and symptoms. *Neuron* 107, 22–37. <https://doi.org/10.1016/j.neuron.2020.05.036>.
- Vitale, N., Caumont, A.S., Chasserot-Golaz, S., Du, G., Wu, S., Sciorra, V.A., Morris, A.J., Frohman, M.A., Bader, M.F., 2001. Phospholipase D1: a key factor for the exocytotic machinery in neuroendocrine cells. *EMBO J.* 20, 2424–2434. <https://doi.org/10.1093/emboj/20.10.2424>.
- Wang, Z., Zhang, F., He, J., Wu, P., Tay, L.W.R., Cai, M., Nian, W., Weng, Y., Qin, L., Chang, J.T., McIntire, L.B., Di Paolo, G., Xu, J., Peng, J., Du, G., 2017. Binding of PLD2-generated phosphatidic acid to KIF5B promotes MT1-MMP surface trafficking and lung metastasis of mouse breast cancer cells. *Dev. Cell* 43, 186–197. <https://doi.org/10.1016/j.devcel.2017.09.012> e7.
- Waselle, L., Gerona, R.R.L., Vitale, N., Martin, T.F.J., Bader, M.-F., Regazzi, R., 2005. Role of phosphoinositide signaling in the control of insulin exocytosis. *Mol. Endocrinol.* 19, 3097–3106. <https://doi.org/10.1210/me.2004-0530>.
- Walter, A.M., Müller, R., Tawfik, B., Wierda, K.D., Pinheiro, P.S., Nadler, A., McCarthy, A.W., Ziolkiewicz, I., Kruse, M., Reither, G., Rettig, J., Lehmann, M., Haucke, V., Hille, B., Schultz, C., Sørensen, J.B., 2017. Phosphatidylinositol 4,5-bisphosphate Optical Uncaging Potentiates Exocytosis *Elife*, vol. 6, e30203. <https://doi.org/10.7554/eLife.30203>.
- Wegrzyn, J.L., Bark, S.J., Funkelstein, L., Mosier, C., Yap, A., Kazemi-Esfarjani, P., La Spada, A.R., Sigurdson, C., O'Connor, D.T., Hook, V., 2010. Proteomics of dense core secretory vesicles reveal distinct protein categories for secretion of neuroeffectors for Cell–Cell communication. *J. Proteome Res.* 9, 5002–5024. <https://doi.org/10.1021/pr1003104>.
- Wu, L., Courtney, K.C., Chapman, E.R., 2021. Cholesterol stabilizes recombinant exocytic fusion pores by altering membrane bending rigidity. *Biophys. J.* 120 (8), 1367–1377. <https://doi.org/10.1016/j.bpj.2021.02.005>.
- Zegarlińska, J., Piascik, M., Sikorski, A.F., Czogalla, A., 2018. Phosphatidic acid - a simple phospholipid with multiple faces. *Acta Biochim. Pol.* 65, 163–171. <https://doi.org/10.18388/abp.2018.2592>.
- Zeniou-Meyer, M., Liu, Y., Bégli, A., Olanich, M.E., Olanish, M., Hanauer, A., Becherer, U., Rettig, J., Bader, M.-F., Vitale, N., 2008. The Coffin-Lowry syndrome-associated protein RSK2 is implicated in calcium-regulated exocytosis through the regulation of PLD1. *Proc. Natl. Acad. Sci. U.S.A.* 105, 8434–8439. <https://doi.org/10.1073/pnas.0710676105>.
- Zeniou-Meyer, M., Zabari, N., Ashery, U., Chasserot-Golaz, S., Haeberlé, A.-M., Demais, V., Bailly, Y., Gottfried, I., Nakanishi, H., Neiman, A.M., Du, G., Frohman, M. A., Bader, M.-F., Vitale, N., 2007. Phospholipase D1 production of phosphatidic acid at the plasma membrane promotes exocytosis of large dense-core granules at a late stage. *J. Biol. Chem.* 282, 21746–21757. <https://doi.org/10.1074/jbc.M702968200>.